

APPENDICES

CHAPTER XI

THE DYNAMIC TEST BENCH

Plate 11.1 illustrates the dynamic test bench employed which is schematically shown in fig. 11.1 .

A 440-V, 3 phase, 50 H_z supply is switched on by the main contactors to the two sets of variable impedances. The first set represents the variable source impedance(0 to 144 ohms- variation in close steps with maximum X/R ratio of 50). The second set of impedances represents the transmission line (impedance variable from 0 to 7 ohms with phase angle setting between 60° and 80°).

For switching ON and OFF the fault, a sequence timer-cum-controlled switching unit is employed. It can initiate the fault at any particular preset angle on the voltage wave. The system fault current and voltage are derived from the bench by current and potential transformers respectively having adequate transformation ratios .

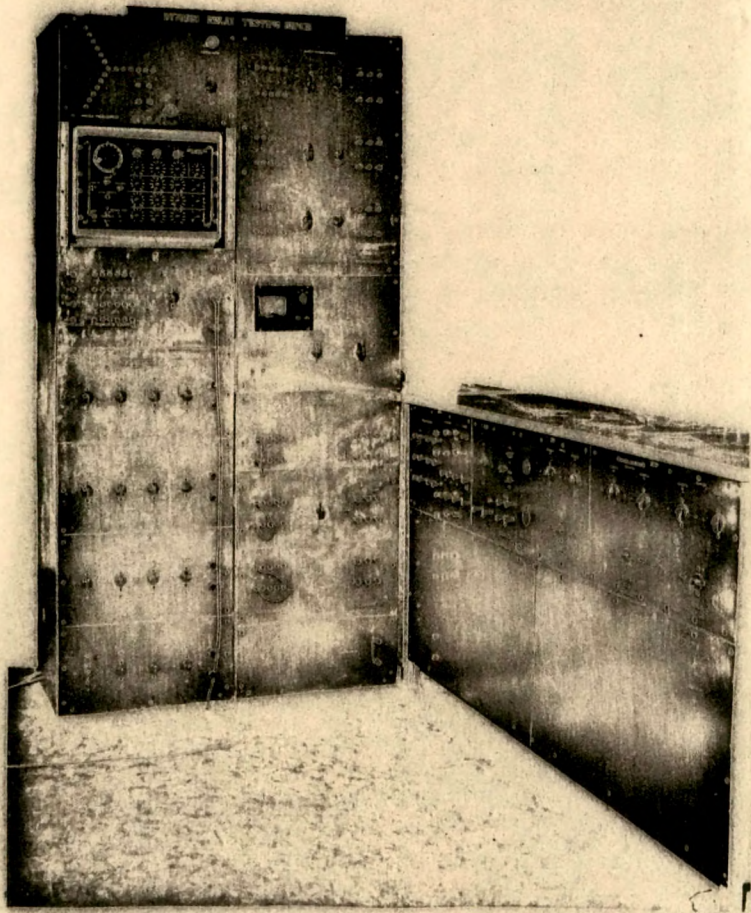
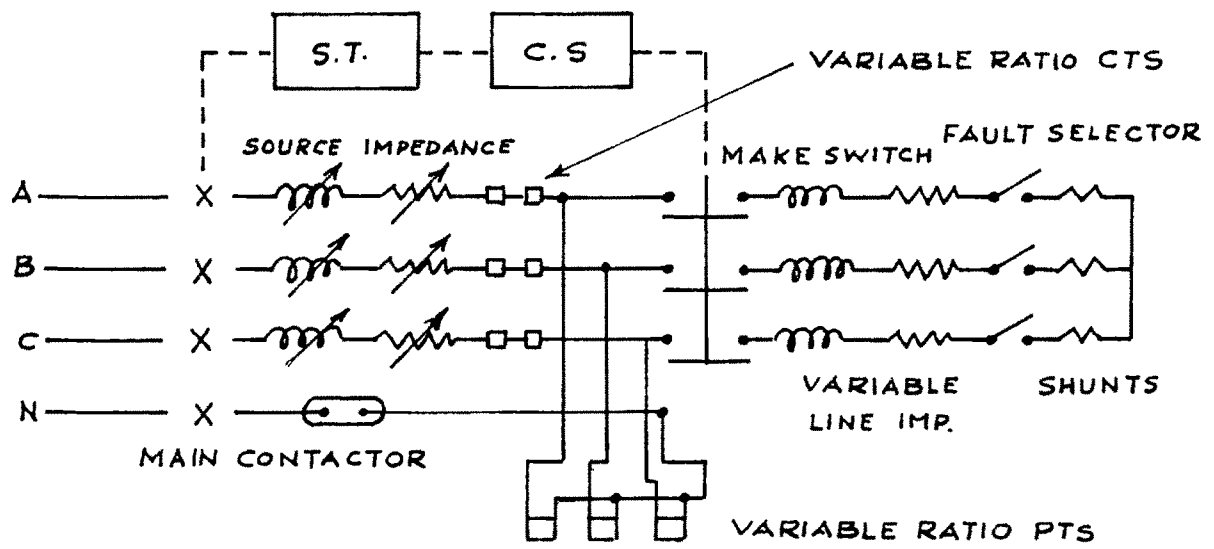


Plate 11.1 Dynamic Relay Testing Bench



S.T. - SEQUENCE TIMER
 C.S. - CONTROLLED SWITCHING UNIT.

FIG. 11-1 DYNAMIC TEST BENCH

CHAPTER XII

TESTING OF THE RELAY EMPLOYING MULTI-INPUT SINE COMPARATOR

Dynamic P-polar Curve :

The following procedure was adopted to obtain the dynamic polar curve of the relay.

Source impedance of the bench was selected as 144 ohms with X/R Ratio of 50. Line impedance was selected as $3 \angle 70^\circ$ ohms. The relay was arranged as a phase fault element utilising the delta voltages and the difference of phase currents. Fault current obtained as shown in fig.12.1 was passed through a replica impedance of 18 ohms with impedance angle of 45° . A C.T. ratio of 5:1 was employed. The fault voltage derived from the bench was applied to the relay through a phase-shifter and a variac.

It may be noted that the replica impedance reflected in the line is less than 1 ohm. The source to line impedance ratio is, therefore, around 40 .

The phase angle between V_L and I_L was varied by the phase shifter. For each setting of the angle between V_L and I_L , the fault was thrown on the line at $\theta_s = 180^\circ$ on the voltage wave. The output pulse of the relay was

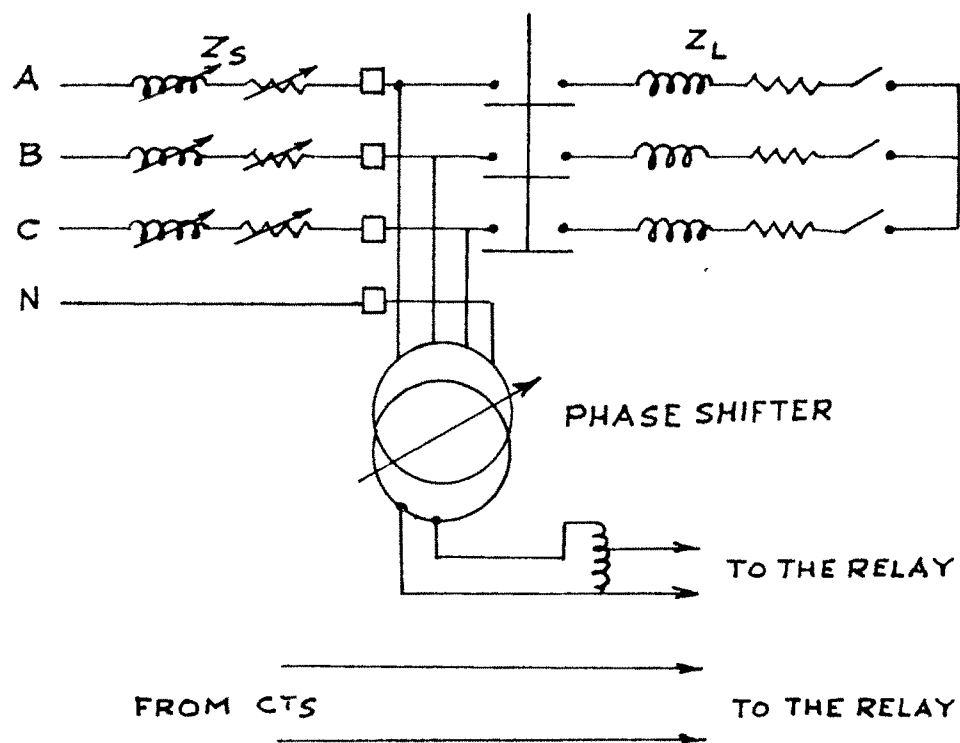


FIG. 12-1 DYNAMIC TEST ARRANGEMENT

observed on C.R.O. For each phase angle, V_L and I_L were measured at the time when the tripping pulse was just on the verge of disappearing in the very cycle after the initiation of the fault.

For each value of the phase angle, V_L and I_L were also measured for the static polar curve. For each observation, the fault was thrown on the line for time long enough to ensure steady-state conditions.

The steady-state and dynamic polar curves obtained during the investigation are presented in fig.12.2. It may be noted that the transient over-reach is less than 6 percent.

Transient Over-reach V/s angle of Switching :

Over and above the dynamic polar curve, the transient over-reach as a function of angle of switching is usually required in predicting the performance of a relay. For this test, therefore, the phase angle between V_L and I_L was selected as 60° . Faults were initiated at different angles on the voltage wave. For each angle of switching, the steady state and dynamic observations of V_L and I_L were recorded. The curve of percentage transient over reach V/s angle of switching obtained during the investigation is presented in fig.12.3 .

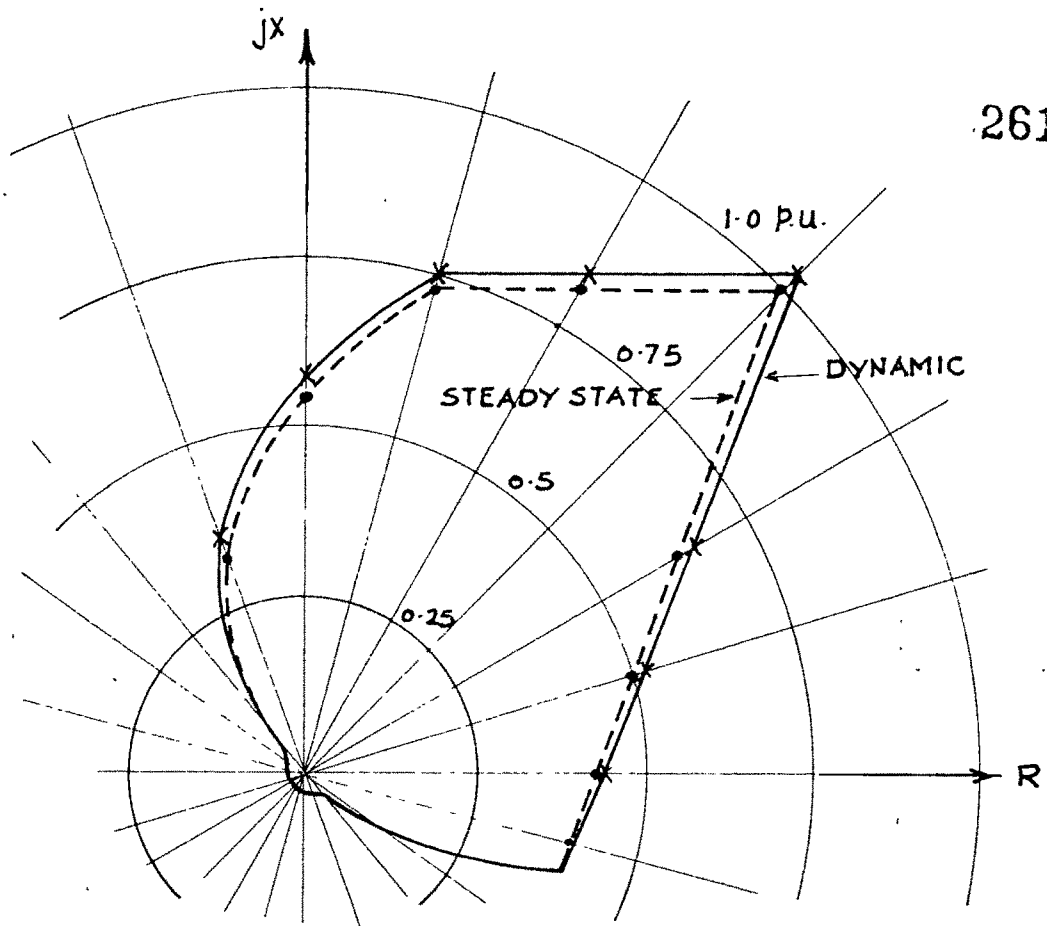


FIG. 12-2 DYNAMIC POLAR CURVE

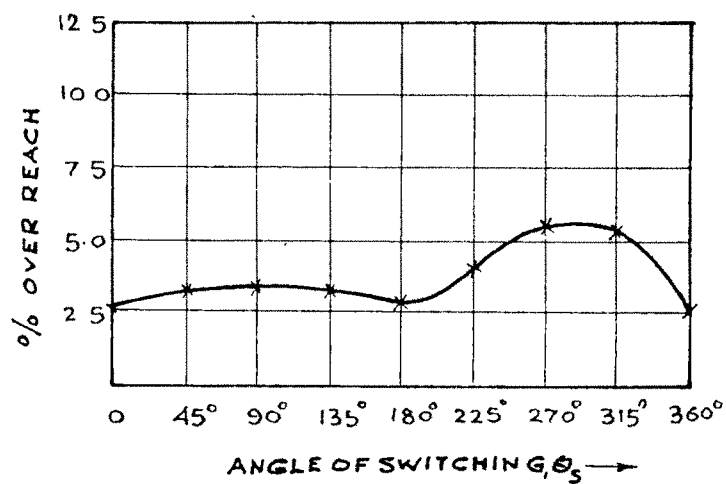


FIG. 12-3 TRANSIENT OVER-REACH V/S ANGLE OF SWITCHING

CHAPTER XIII

TESTING OF HYBRID COMPARATOR

YIELDING CONIC CHARACTERISTICS

The hybrid comparator described in chapter V was arranged to provide various conic characteristics. The comparator was tested during steady-state conditions only. Fig.13.1 illustrates the basic set-up of the testing.

System quantities I_L and V_L were obtained from the primary and secondary windings respectively of a 3-phase phase shifter. A replica impedance with impedance angle of 70° was introduced in the measuring circuits. Signals $I_L Z_R$ and V_L were applied to the relay through separate variacs. The phase angle between V_L and I_L was varied by means of the phase shifter. For each setting of the angle between V_L and I_L , V_L was varied keeping I_L constant. Both V_L and I_L were measured at the time when the output tripping pulse was just on the verge of disappearing. Z_L was then calculated and plotted against ϕ . The various conic characteristics so obtained are presented in fig.13.2 through 13.4 .

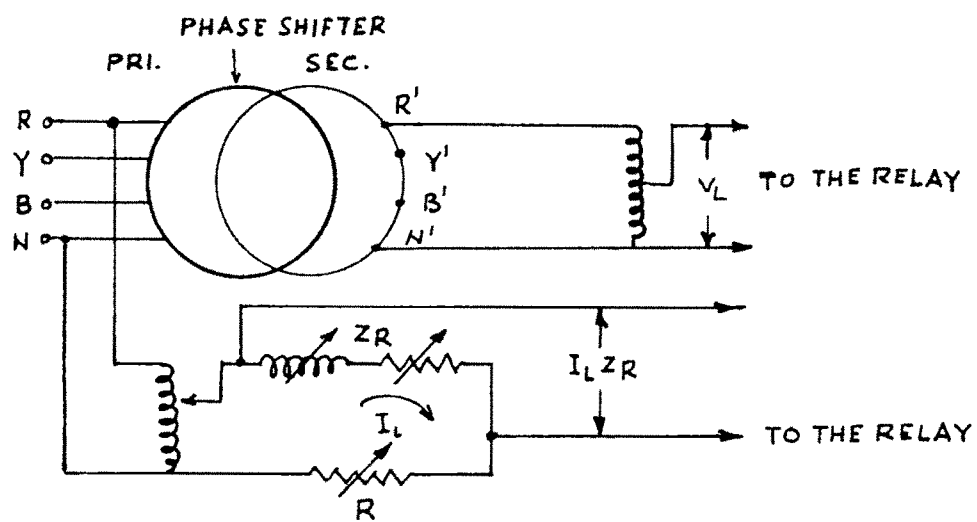
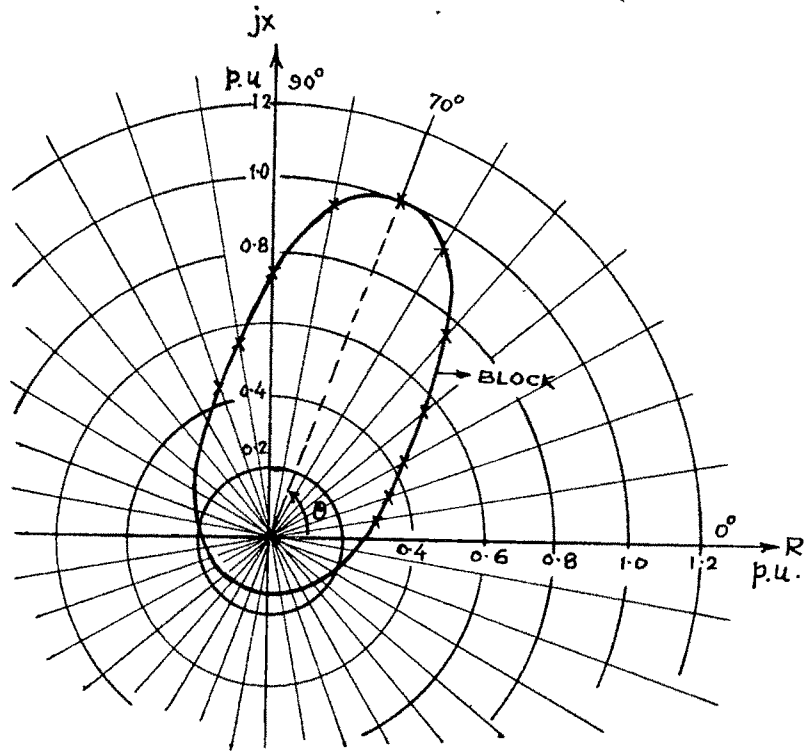
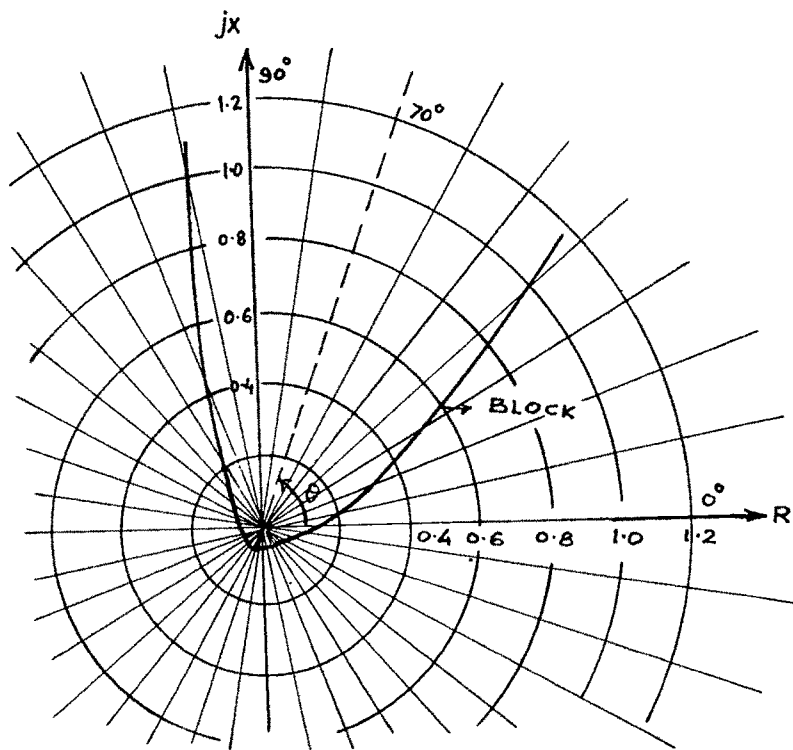


FIG. 13-1 TESTING SET-UP

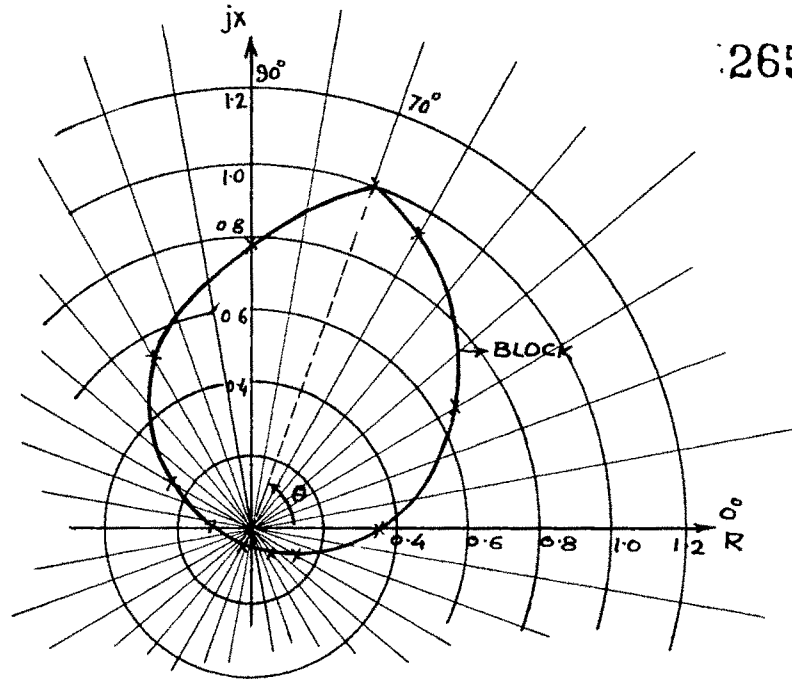


(a) ELLIPSE

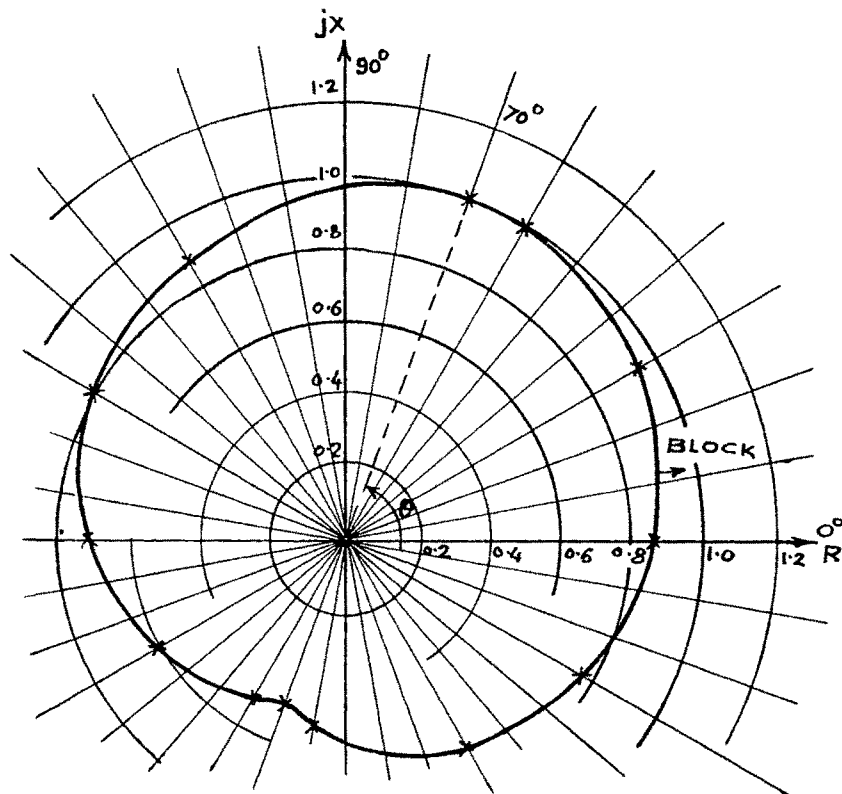


(b) PARABOLA

FIG. 13.2 STEADY-STATE CONIC CHARACTERISTICS



(a) LIMACON ($b < a$)



(b) LIMACON ($b > a$)

FIG. 13-3 STEADY-STATE CONIC-CHARACTERISTICS

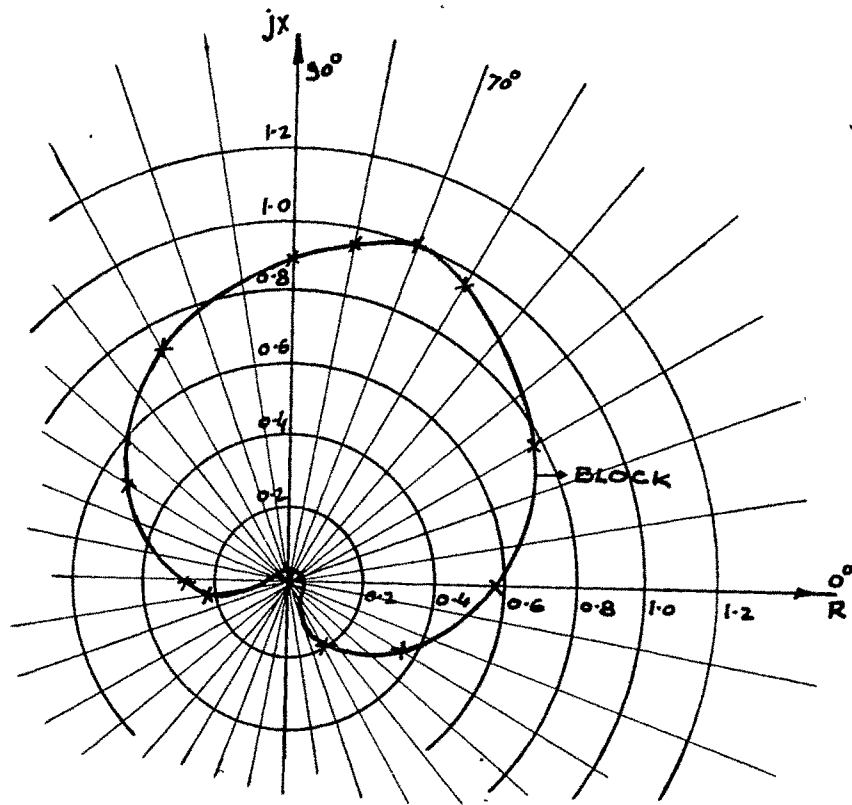


FIG. 13-4 STEADY-STATE CARDIOID

CHAPTER XIV

RESULTS OF COMPUTER PROGRAMMES AND TESTS CONDUCTED

ON THE COMPARTOR YIELDING SELF-ADJUSTING CHARACTERISTIC

Ratios V_b / E_p for Line To Ground Faults On Phase A

In running the programme on Digital Computer following system data was assumed :

$$\text{Total Line Impedance : } Z_1 = (0.08 + j0.241)\text{p.u.}$$

$$Z_0 = (0.2 + j0.72) \text{ p.u.}$$

$$\text{Machine Impedances : } Z_{A1} = Z_{A2} = j0.35 \text{ p.u.}$$

$$Z_{A0} = j0.15 \text{ p.u.}$$

$$Z_{B1} = Z_{B2} = j0.3 \text{ p.u.}$$

$$Z_{B0} = j0.05 \text{ p.u.}$$

$$\text{Transformer Impedances: } Z_T = j0.12 \text{ p.u.}$$

The fault resistance was assumed to be 0.055 p.u.
 C_0 and C were varied between 0.2 and 1.0 for the selected locations of the fault. The ratios V_b / E_p so obtained are tabulated in Table 1.

Table 1

Sr. No.	Fault Location m	C_o	C	V_b / E_p
1	0.1	0.2	0.2	0.9838
2	0.1	0.4	0.4	0.9847
3	0.1	0.6	0.6	0.9856
4	0.1	0.8	0.8	0.9865
5	0.1	1.0	1.0	0.9873
6	0.5	0.2	0.2	0.9999
7	0.5	0.4	0.4	1.0032
8	0.5	0.6	0.6	1.0065
9	0.5	0.8	0.8	1.0098
10	0.5	1.0	1.0	1.0130
11	0.9	0.2	0.2	0.9388
12	0.9	0.4	0.4	0.9589
13	0.9	0.6	0.6	0.9793
14	0.9	0.8	0.8	1.0001
15	0.9	1.0	1.0	1.0213

Determination of K_1

Initially to determine C_1 , θ was selected equal to $(\theta-90^\circ)$. V_L was varied in steps. For different values of V_L , both $|V_L|$ and peak amplitude of e_{c_1} were measured and recorded. C_1 was then calculated and tabulated as shown in

Table 2. From table 2 it is evident that the average value of C_1 is 0.209.

Table 2

Sr. No.	$ V_L $ Volts	e_{c_i} Volts	$C_1 = e_{c_i}/ V_L $	C_1 Average
1	4.8	1.0	0.208	0.209
2	6.8	1.4	0.206	0.209
3	8.6	1.9	0.221	0.209
4	11.0	2.2	0.200	0.209

To determine the gain of the A.G.C. amplifier \emptyset was selected equal to 0^0 . V_L was varied in steps. For different values of V_L , the peak amplitudes of e_{c_i} , e_c and $|V_L|$ were recorded. From these observations, the stage gain was calculated and the corresponding values of K_1 were determined. These values are presented in Table 3.

Table 3

Sr. no.	$ V_L $ in p.u.	K_1
1	0.0	0.0
2	0.218	0.006
3	0.327	0.038
4	0.46	0.052
5	0.605	0.1
6	0.715	0.166
7	0.788	0.25
8	0.908	0.344
9	1.0	0.416

Effect Of The Location Of The Fault And Z_S/Z_L
Ratio On The Shape Of The Characteristic :

From fig.7.11 the p.u. voltage at the relay location may be written as

$$\left| \frac{V}{E} \right| = \frac{m}{(Z_S / Z_L)^m + m} \quad \dots (14.1)$$

To appreciate the effects of fault location and source/line impedance ratio, a computer programme was run using equations (7.3), (7.13) and (14.1). The values of K_2 and K_3 were selected on the basis described in section 7.6.2.

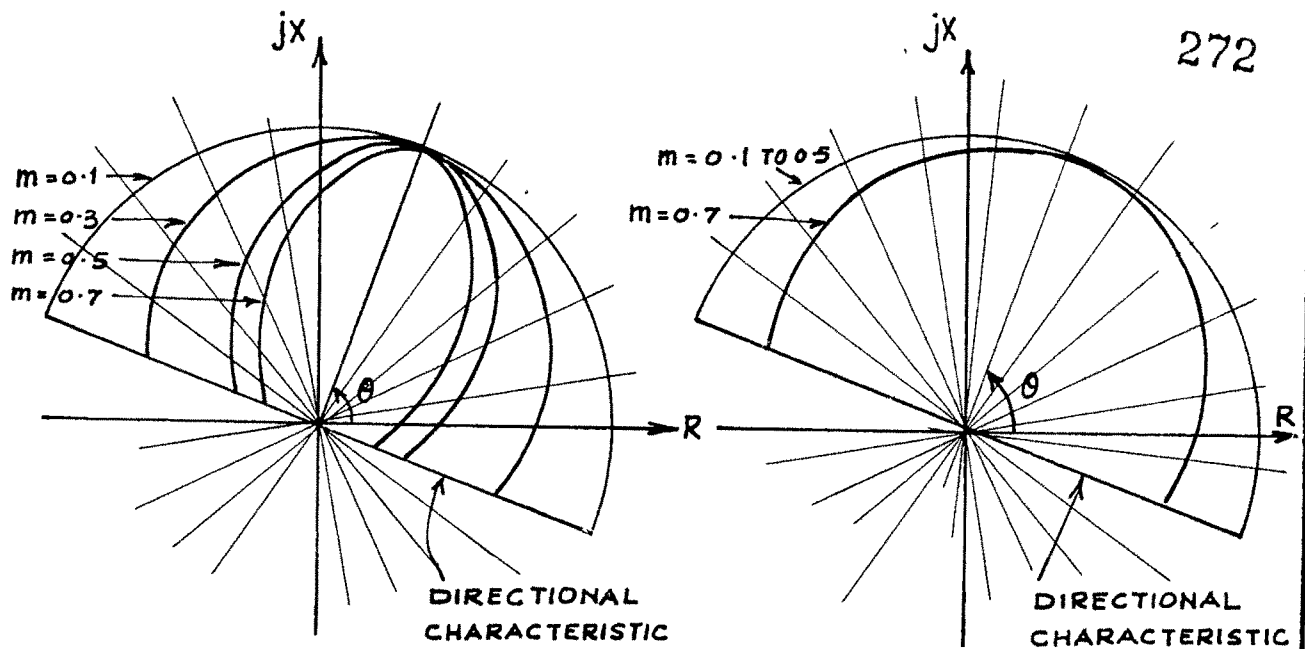
The negative values of K_1 obtained from equation 7.13 for low values of $|V/E|$ were converted to zero to take into account the physical behaviour of A.G.C. during such conditions. The factor m was varied from 0.1 to 0.7 alongwith the variation of Z_S / Z_L from 1.0 to 40.0 in steps. The characteristics obtained from the programme are shown in fig. 14.1 .

From fig.14.1 it is evident that for low source/line impedance ratios the characteristics are elliptical, their eccentricity being decreasing for decreasing values of m . For larger source/line impedance ratios the self-adjusting characteristic assumes the shape of the plain impedance characteristic for all possible locations of the fault in the protected section.

Steady State And Dynamic Testing :

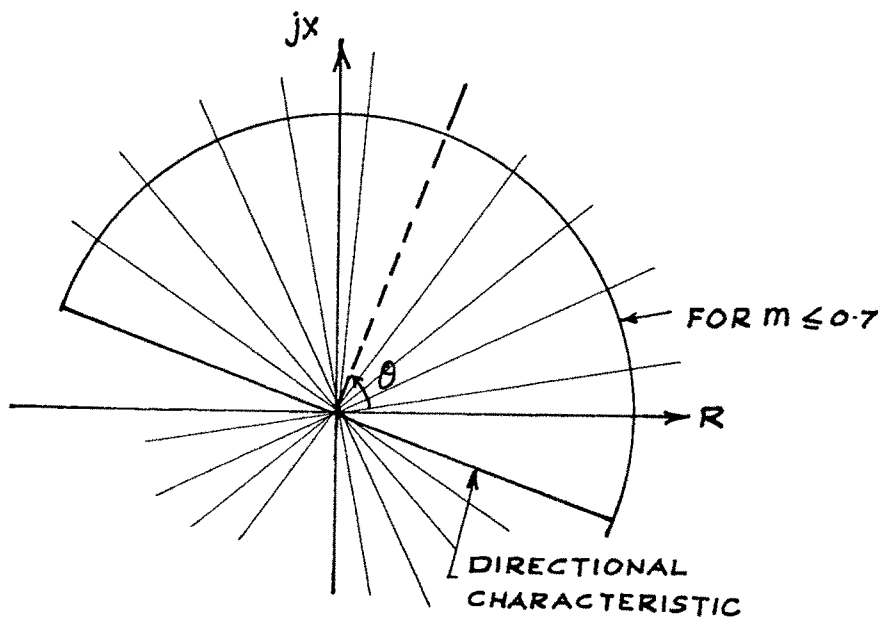
Static Polar Curves :

To obtain the static polar curves of the relay the set-up was made as shown in fig.13.1 . Signals I_L and V_L were obtained from the respective primary and secondary windings of the phase-shifter. A replica impedance with impedance angle of 70° was introduced in the measuring circuit. $I_L Z_R$ and V_L were applied to the relay through separate variacs. Since the shape of the characteristic depends upon the value of V_L , it was necessary to keep V_L



(a) $Z_s/Z_L = 1.0$

(b) $Z_s/Z_L = 2.5$



(c) $Z_s/Z_L > 10.0$

FIG. 14.1 SELF ADJUSTING CHARACTERISTICS

constant and vary I_L . For each setting of the angle between V_L and I_L , therefore, V_L was kept constant and I_L was varied to obtain the tripping characteristics. With different values of V_L , the characteristics so obtained are presented in fig. 14.2 .

Transient Over-reach :

To determine the transient performance of the relay the dynamic test bench described in chapter XI was employed. The source impedance of the bench was selected as 14 Ω ohms, with X/R ratio of 50. Line impedance was selected as 3 $\angle 70^\circ$ ohms . Fault current obtained from the bench was passed through a replica impedance of 10 ohms with impedance angle of 70° . A C.T. ratio of 5:1 was employed. The fault voltage derived from the bench was applied to the relay through a phase shifter and a variac.

As mentioned above it was necessary to keep V_L constant and vary I_L in determining the transient performance of the relay. However, it was not possible in the test bench to vary I_L continuously. ϕ was therefore selected equal to θ , for which the impedance seen by the relay has the same value for all values of V_L .

At the end of the line, faults were thrown at different angles on the voltage wave. For each angle of switching, the steady state and dynamic observations of

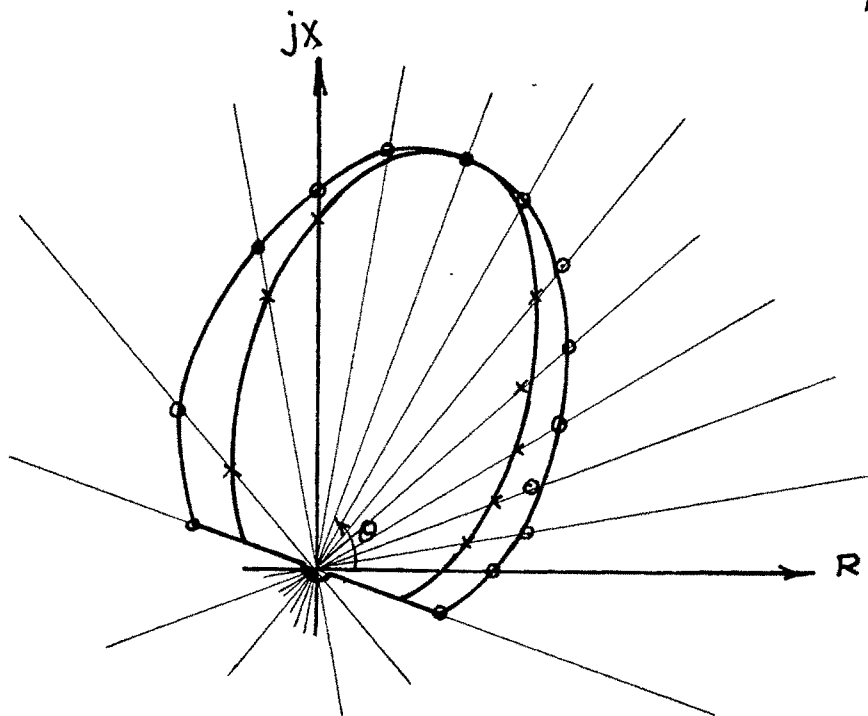


FIG. 14.2 STATIC POLAR CURVES

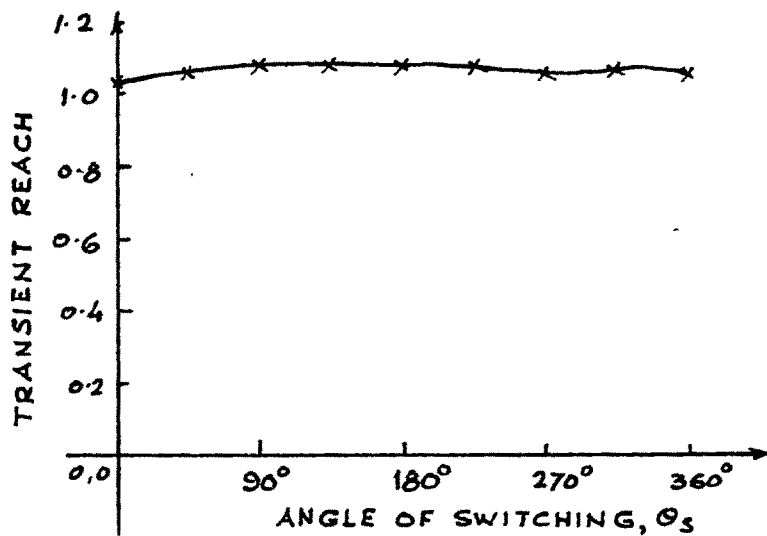


FIG. 14.3 OVER REACH FACTOR V/S ANGLE
OF SWITCHING.

V_L and I_L were recorded. The curve of transient reach against the angle of switching obtained during the investigation is presented in fig.14.3 .

Time Contour Curves :

The time contour curves of the hybrid comparator are determined and presented in fig.14.4 and 14.5 . The contour curves are presented up to a system impedance ratio of 40 . This is because, that for E.H.V. systems using high capacity generating units, the system impedance ratio may not go beyond 10 during light load conditions. These figures represent the constant operating time characteristics for zero and maximum transients for a line to line fault between phases Y and B . It can be seen that the basic operating time is about 20 m sec. and, as is inherent in all distance schemes, the operating time varies slightly depending upon the position of fault and the magnitude of fault current and voltage. The figures also indicate that fast operation is maintained over the entire zone down to very low voltages. Further, it is evident that the offset d.c. transient components of the current do not unduly affect the operation of relay for the entire range.

Plates 14.1 through 14.6 show the current wave forms and the time of occurrence of the tripping pulse for different Y, X and the angles of switching.

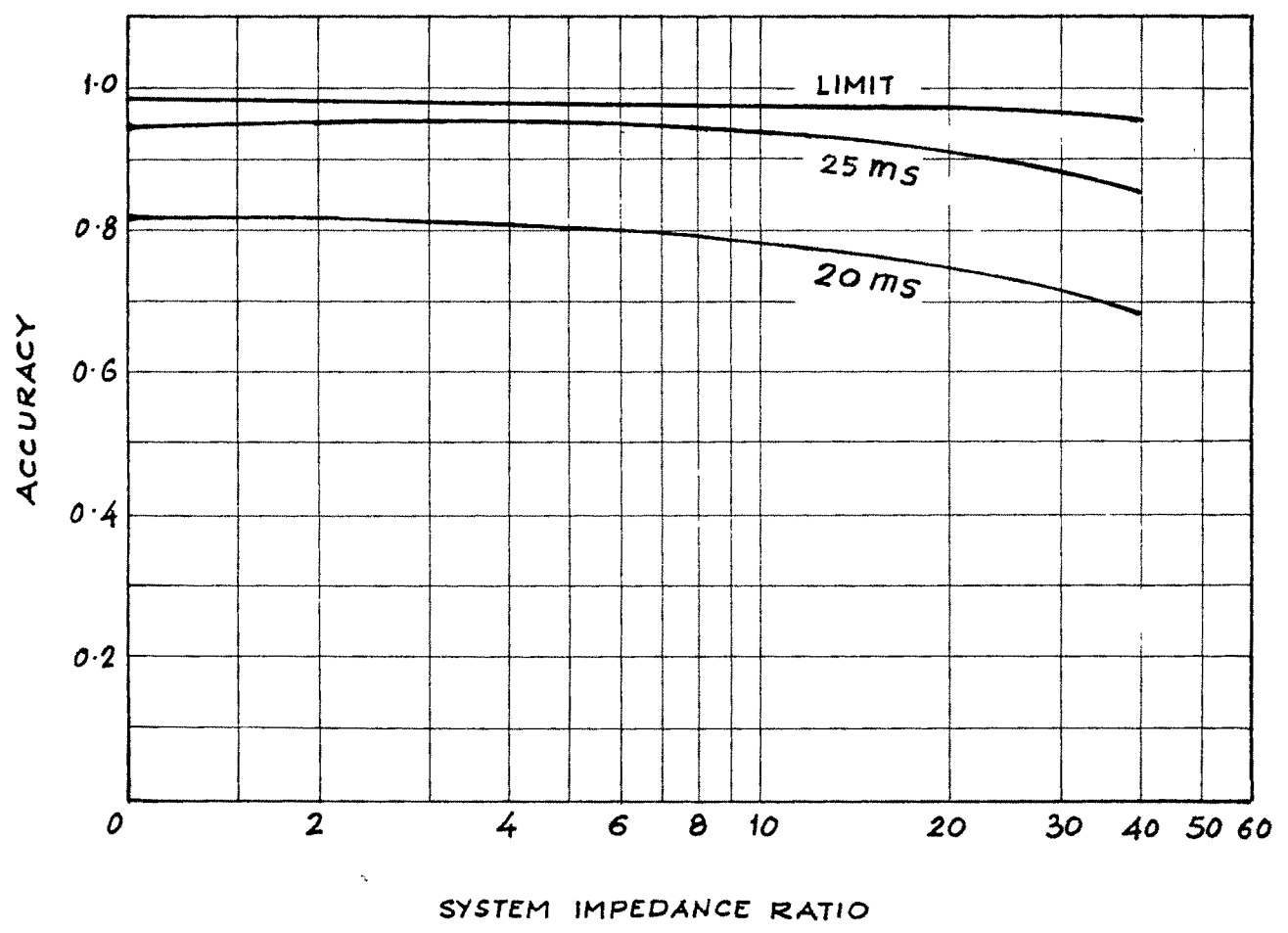


FIG. 14.4 TIME CONTOURS FOR HYBRID COMPARATOR
(PHASE FAULT Y-B)
ZERO TRANSIENT

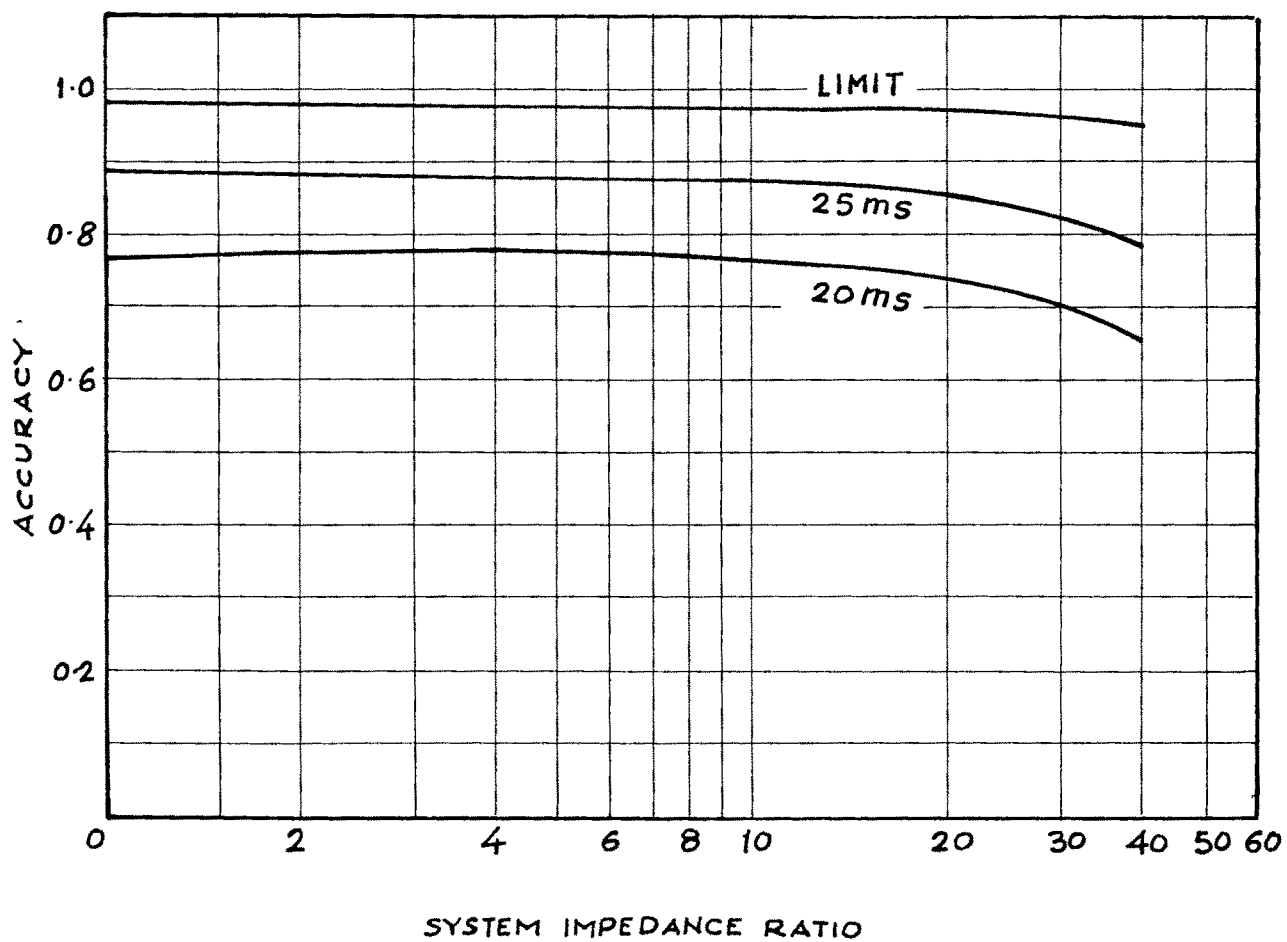


FIG.14.5 TIME CONTOURS FOR HYBRID COMPARATOR
(PHASE FAULT Y-B)
MAXIMUM TRANSIENT

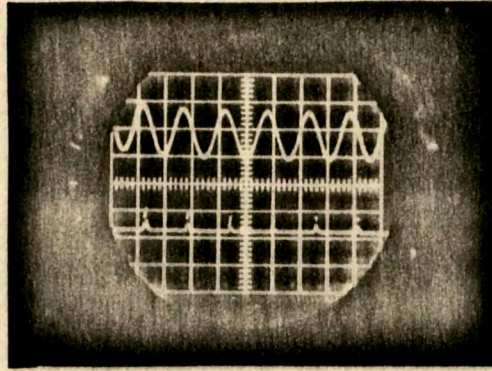


Plate 14.1 Current Oscillogram

$\theta_s = 45^\circ$; $Y = 14.4$;
 $X = 0.7$

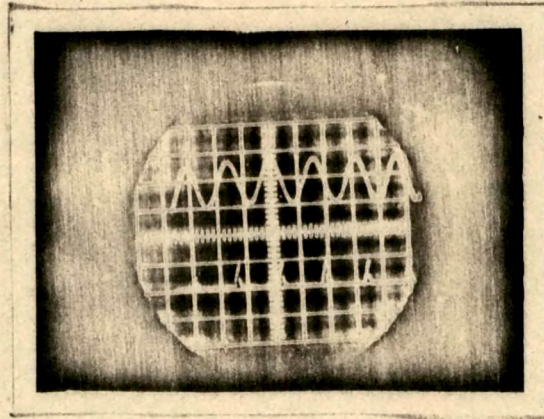


Plate 14.2 Current Oscillogram

$\theta_s = 0^\circ$; $Y = 14.4$
 $X = 0.5$

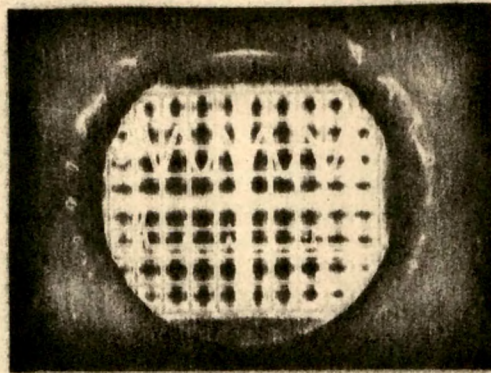


Plate 14.3 Current Oscillogram

$$\theta_s = 90^\circ ; Y = 14.4 ; \\ X = 0.5$$

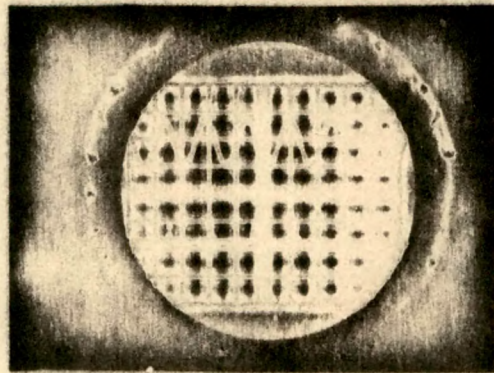


Plate 14.4 Current Oscillogram

$$\theta_s = 45^\circ ; Y = 22.1 ; \\ X = 0.5$$

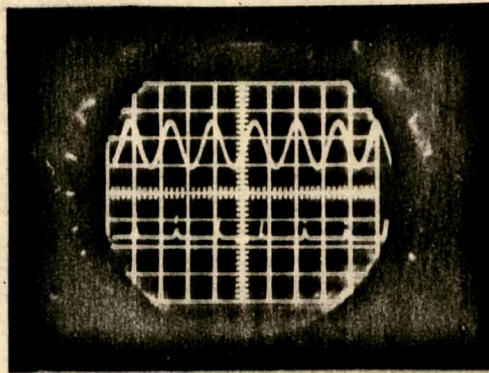


Plate 14.5 Current Oscillogram

$$\theta_s = 180^\circ ; Y = 22.1 ; \\ X = 0.8$$

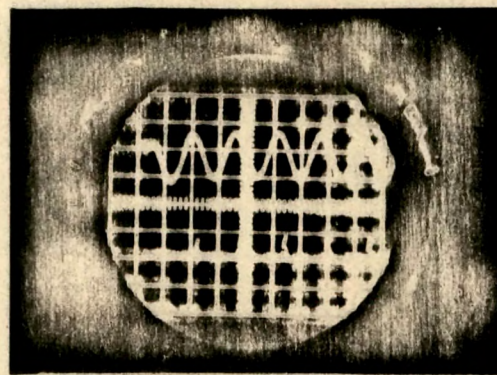


Plate 14.6 Current Oscillogram

$$\theta_s = 270^\circ ; Y = 14.4 ; \\ X = 0.5$$

CHAPTER XV

INPUT ADMITTANCE DIAGRAM FOR A 4-TERMINAL NETWORK

A typical 4-terminal network ⁵⁴ having constants, A, B, C, D is shown in fig.15.1 . The necessary expressions for sending end voltage and currents are :

$$V_S = A V_R + B I_R \quad \dots (15.1)$$

$$I_S = C V_R + D I_R \quad \dots (15.2)$$

where, $A = 1 + Y_R Z$; $B = Z$; $C = Y_R + Y_S + Y_R Y_S Z$ and

$$D = 1 + Y_S Z$$

If V_R is fixed and V_S is varied in phase and magnitude, then ,

$$V_S = K V_R \angle \delta \quad \dots (15.3)$$

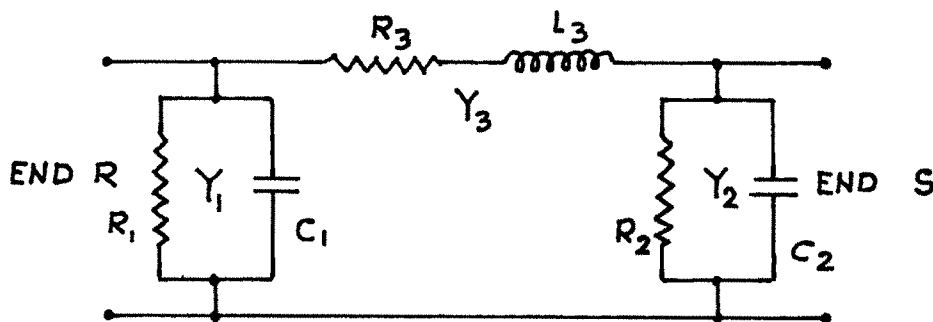
where $K = | V_S | / | V_R |$. δ is the angular difference between the two voltages.

From eq.(15.1) through (15.3) ,

$$Y_{PR} = \frac{I_R}{V_R} = \frac{K \angle \delta - A}{B} \quad \dots (15.4)$$

To take into account the current at end R to enter in the network eq.(15.4) must be multiplied by -1, giving

$$Y_{PR} = \frac{A - K \angle \delta}{B} \quad \dots (15.5)$$



$$R_1 = 22.5 \text{ k}\Omega$$

$$C_1 = 0.864 \mu\text{F}$$

$$R_2 = 30.3 \text{ k}\Omega$$

$$C_2 = 0.804 \mu\text{F}$$

$$R_3 = 2.33 \text{ k}\Omega$$

$$L_3 = 3.03 \text{ H}$$

$$Y_1 = (A-1)/B$$

$$Y_2 = (D-1)/B$$

$$Y_3 = 1/B$$

FIG. 15.1 EQUIVALENT T NETWORK FOR A TYPICAL
25-MILE LONG PRACTICAL PILOT-CIRCUIT

The locus of Y_{PR} given by eq.(15.5) is a series of circles of radius K/B at a distance A/B ($A/B = Y_{SCR}$, the short circuit admittance viewed from end R) from the centre of the admittance plane (as shown in fig.8.1) .

CHAPTER XVI

DERIVATION OF PROPAGATION CONSTANT

Fig.16.1 shows an equivalent circuit of pilot-wires .
 Y_{r1} and Y_{r2} are the relay burdens on pilot-wires. Let E_1
be the voltage received at station 1 from station 2 over
the pilot-wires.

From fig.16.1 , the following expressions for E_1''
can be written ,

$$\begin{aligned} E_1'' &= E_1 + E_1 (Y_{r1} + Y_1) B \\ &= E_1 [1 + (Y_{r1} + Y_1) B] \end{aligned}$$

$$\begin{aligned} \therefore E_1 &= \frac{E_1''}{1 + (Y_{r1} + Y_1) B} \\ &= \delta E_1'' \end{aligned}$$

$$\text{where } \delta = \frac{1}{1 + (Y_{r1} + Y_1) B} \quad \dots (16.1)$$

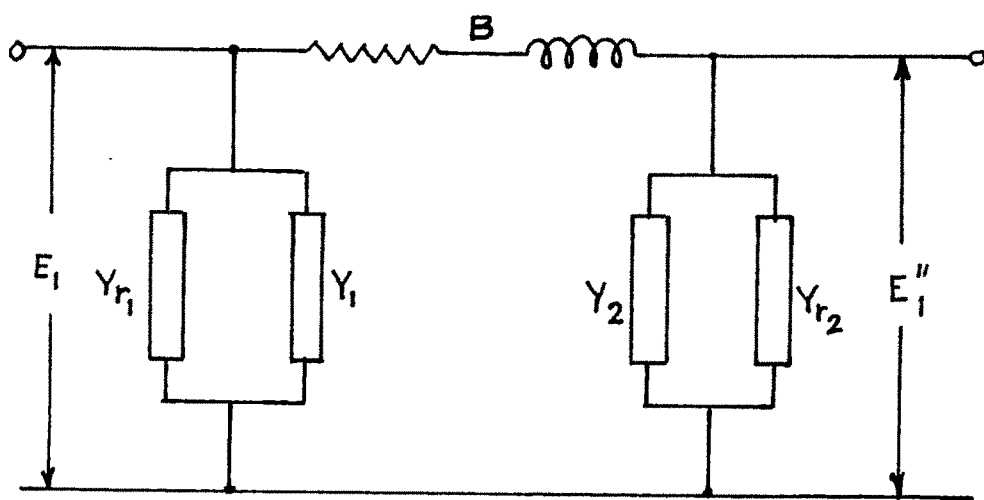


FIG. 16-1 EQUIVALENT CIRCUIT OF PILOT-WIRES